

Frequency Dependence of the Drifting Sub-Pulses of PSR B0031–07 †

J. M. Smits¹ ★, D. Mitra² and J. Kuijpers¹

¹ Department of Astrophysics, Radboud University Nijmegen, Nijmegen, The Netherlands

² National Center for Radio Astrophysics, Pune, India

Abstract The well known drifter PSR B0031–07 is known to exhibit drifting sub-pulses where the spacing between the drift bands (P_3) shows three distinct modes A, B and C corresponding to 13, 7 and 4 times the pulsar period, respectively. We have investigated periodicities and polarisation properties of PSR B0031–07 for a sequence of 2700 single pulses taken simultaneously at 328 MHz and 4.85 GHz. We found that mode A occurs simultaneously at these frequencies, while modes B and C only occur at 328 MHz. However, when the pulsar is emitting in mode B at the lower frequency there is still emission at the higher frequency, hinting towards the presence of mode B emission at a weaker level. Further, we have established that modes A and B are associated with two orthogonal modes of polarisation, respectively. Based on these observations, we suggest a geometrical model where modes A and B at a given frequency are emitted in two concentric rings around the magnetic axis with mode B being nested inside mode A.

Key words: stars: neutron — pulsars: general — pulsars: individual (B0031–07)

1 INTRODUCTION

The single pulses of a pulsar are known to be composed of several smaller units of emission called sub-pulses. These sub-pulses are often seen to drift in phase across a sequence of single pulses giving rise to the well-known phenomenon of ‘drifting sub-pulses’, discovered in 1968 (Drake & Craft 1968). The drift pattern is seen to repeat itself after a given time which is usually denoted by P_3 . The phenomenon has since been detected in many pulsars (e.g. Rankin 1986) and the process is believed to carry information on the mechanism leading to coherent radio emission from pulsars.

PSR B0031–07 shows three distinct drift modes with different P_3 , which are all very stable. They are named mode A, B and C and correspond to a P_3 of 13, 7 and 4 times the pulsar period, respectively. These values are approximations and from 40 000 pulses observed at 327 MHz Vivekanand & Joshi (1997) found that they may not be harmonically related. They also found that at 327 MHz the relative occurrence rate of these modes are 15.6%, 81.8% and 2.6%, respectively. Furthermore, the pulses occur in clusters containing 30 to 100 pulses which follow each other with intervals ranging from fifty to several hundred pulse periods. This pulsar also shows a clear presence of Orthogonally Polarised Modes (OPM) in the integrated position angle sweep (Manchester et al. 1975).

In this paper we study the behaviour of the different modes of drift in PSR B0031–07 in radio observations at both low and high observing frequencies simultaneously and present a geometrical model which describes many of the observed characteristics of this pulsar.

† A complete account of this research can be found in Smits et al. (2005)

★ E-mail: R.Smits@astro.ru.nl

2 DATA ANALYSIS

The observations of PSR B0031–07, were obtained on 3 February 2002 with both the Westerbork Synthesis Radio Telescope (WSRT) and the Effelsberg Radio Telescope simultaneously. These observations were obtained as part of the MFO¹ program. The WSRT observations were made at a frequency of 328 MHz and a bandwidth of 10 MHz. The Effelsberg observations were made at a frequency of 4.85 GHz and a bandwidth of 500 MHz. The time resolutions are 204.8 μ s and 500 μ s for the 328 MHz and 4.85 GHz observations, respectively.

We have also used an observation of PSR B0031–07, obtained on 9 August 1999 with the Effelsberg Radio Telescope at a frequency of 1.41 GHz and a bandwidth of 40 MHz. The time resolution is 250 μ s.

2.1 Calculation of P_3

To search for periodicities, we considered sequences of pulses from the observations. For each pulse in a sequence, we took the flux at a fixed pulse phase, and calculated the absolute values of the Fourier transform of this flux distribution. This was done for each phase of the pulsar window. The resulting transforms were then averaged over phase, giving a phase-averaged power spectrum (PAPS) from 0 up to 0.5 cycles per rotation period (hereafter $c P_1^{-1}$), with a frequency resolution given by the reciprocal of the total length of the sequence.

Initially, all pulses from the observations were divided into sequences of 100 pulses, which were searched for peaks in the PAPS. When a peak was found, the beginning and end of the sequence was adjusted to get the highest signal-to-noise ratio for the peak. The signal-to-noise ratio was calculated as the peak value of the PAPS divided by the rms of the rest of the PAPS. This result was checked by visual inspection of the sequences to see whether they did indeed match the beginning and ending of a drift band. P_3 was then calculated as the reciprocal of the centre of the peak in the PAPS. When a peak would spread over multiple bins, a cubic spline interpolation was used to determine the location of the peak. The frequency resolution, given by the number of pulses in the sequence, was taken as the error on the position of the peak.

Furthermore, we have calculated the PAPS of all pulses of the 1.41- and of the 4.85-GHz observations in order to find signs of 6 second periodicity. For comparison, we also calculated the PAPS of the 328-MHz observation.

2.2 Average Profiles and Polarisation Properties

To further study these distinct periodicities, we looked at the average-pulse profiles from all pulses that show mode-A and mode-B drift, respectively. Since the pulses at 4.85 GHz do not show a mode-B drift, we averaged pulses that showed mode-B drift in the 328-MHz observation to produce the mode-B profile at 4.85 GHz. In the same way, we calculated the average linear polarisation, circular polarisation and position angle as a function of pulse phase.

3 RESULTS AND DISCUSSION

The values of P_3 for each sequence and for both frequencies are shown in Figure 1. The mode-A drift is clearly present at both frequencies, however, the mode-B drift is only visible at 328 MHz. It should be noted that whenever mode B is active at 328 MHz there is always radiation present at 4.85 GHz. The same is true for mode C, but there is only one case of a mode C drift. Figure 1 also suggests that the transition between modes can happen within one or a few pulses.

The PAPS of all three observations, are shown in Figure 2. At low frequencies a signal is present due to the nulling. To make the figure clearer we have set this to zero. We see here that the 6-second periodicity is clearly present at 328-MHz and is just visible in the 1.41-GHz observation. At 4.85 GHz the PAPS does not show the 6-second periodicity. Thus, the mode-B drift gets weaker with increasing observing frequency. However, we did find small sequences in the 4.85-GHz observation where there is a weak 6-second periodicity. This would suggest that towards higher frequency we are seeing less of the drifting sub-pulses and begin to see a diffuse component that is also subject to drift.

Figure 3 shows the average-polarisation properties of pulses which show the same modes of drift: the top panels for mode-A drift, the middle panels for mode-B drift and the lower panels for all pulses. Each

¹ The MFO collaboration undertakes simultaneous multi-frequency observations with up to seven telescopes at any one time.

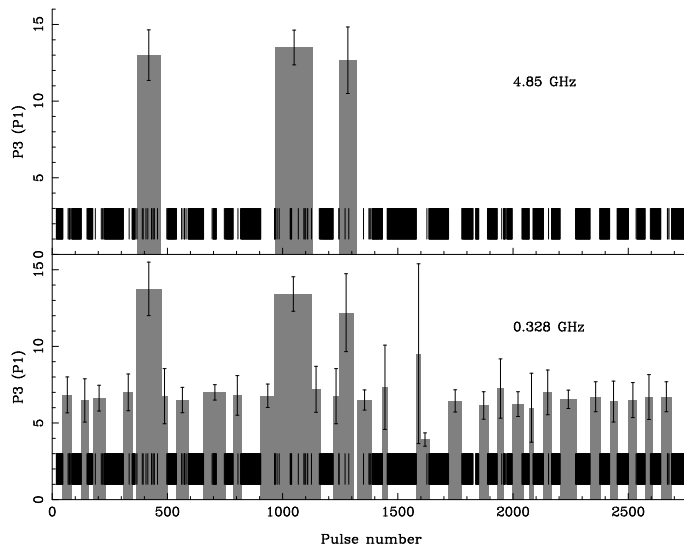


Fig. 1 Sequences which show a periodicity of magnitude P_3 at fixed pulse phase (the gray areas). The lower panel shows the 328 MHz observation, while the upper panel shows the 4.85 GHz observation. The black band indicate pulses which show a null at both frequencies.

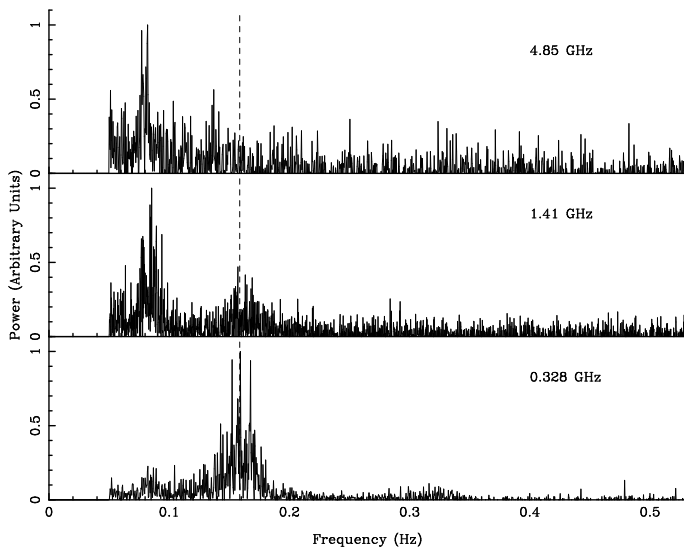


Fig. 2 Phase averaged power spectra of three observations at frequencies of 4.85 GHz, 1.41 GHz and 328 MHz. There are clear signs of 6-second periodicity in the 1.41-GHz and 328-MHz observations. The dotted line is placed at $1/6.3$ s.

panel shows the total intensity (solid line), linear polarisation (dashed line), circular polarisation (dotted line) and position angle (lower half of each panel). The left panels show the 328-MHz profiles, the right panels show the 4.85-GHz profiles. There is a clear 90° jump in the position angles of all pulses in both the 328-MHz and 4.85-GHz profiles at a phase of 24° . This jump can also be seen in the pulses that only show a mode-B drift. At 328 MHz, the A-profile seems to have two components. This can correspond to the line of sight cutting the edge of the sub-pulses in the centre of the profile, thereby bifurcating the average

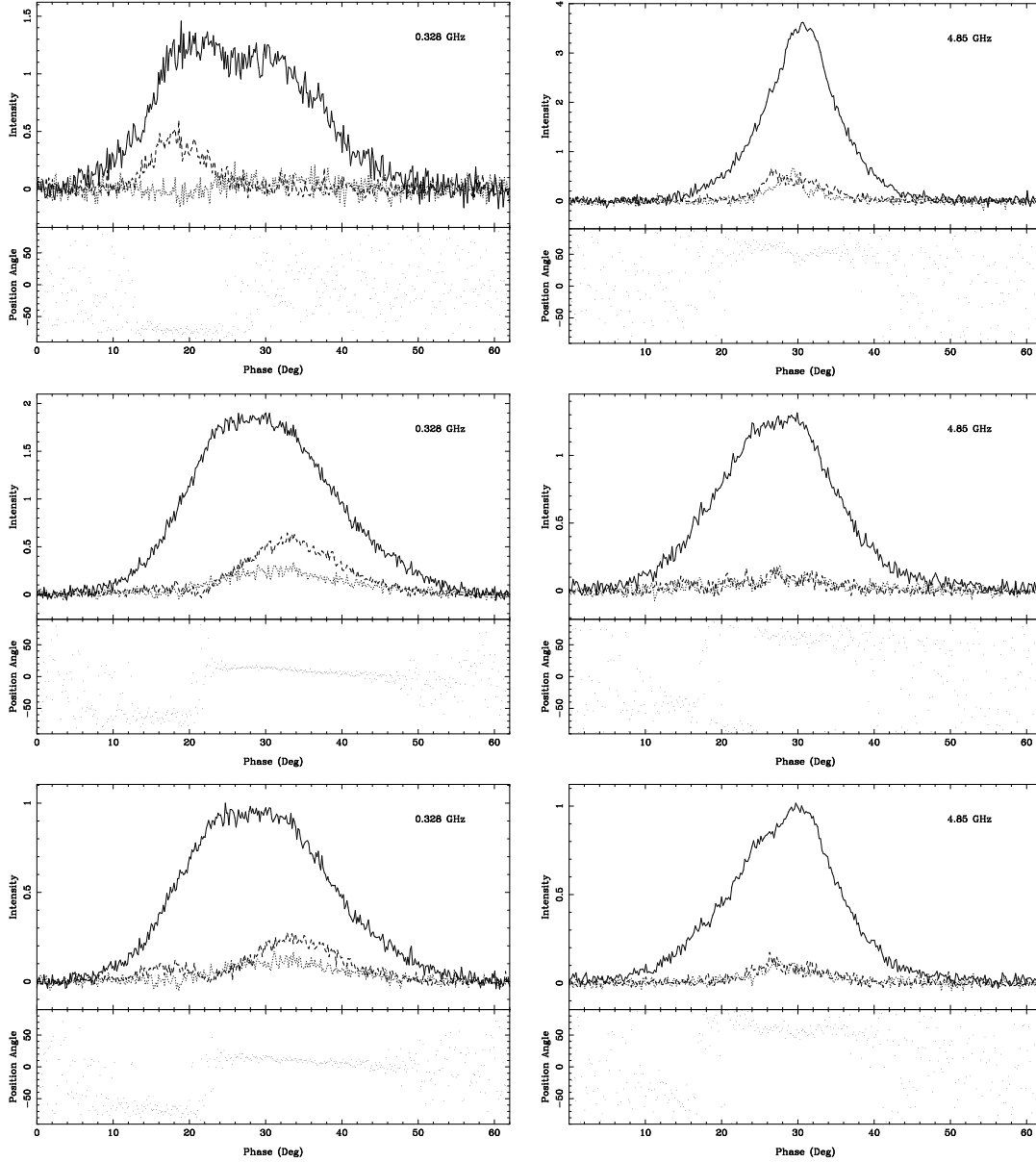


Fig. 3 Average intensity and polarisation of pulses in mode A (top panels), pulses in mode B (middle panels) and all pulses (lower panels). The profiles have been normalised to set the peak in the average intensity of all pulses to 1. The left panels show the average of pulses at 328 MHz, the right panels show the average of the same pulses at 4.85 GHz. Since the pulses at 4.85 GHz do not show a mode-B drift, the right middle panel contains the average of pulses at 4.85 GHz that show a mode-B drift at 328 MHz. The solid, dashed and dotted lines in each panel represent the total intensity, linear polarisation and circular polarisation, respectively. The lower part of the panels show the polarisation position angle. The 328 MHz profiles have been re-binned to $500 \mu\text{s}$ per bin, to make the profiles comparable.

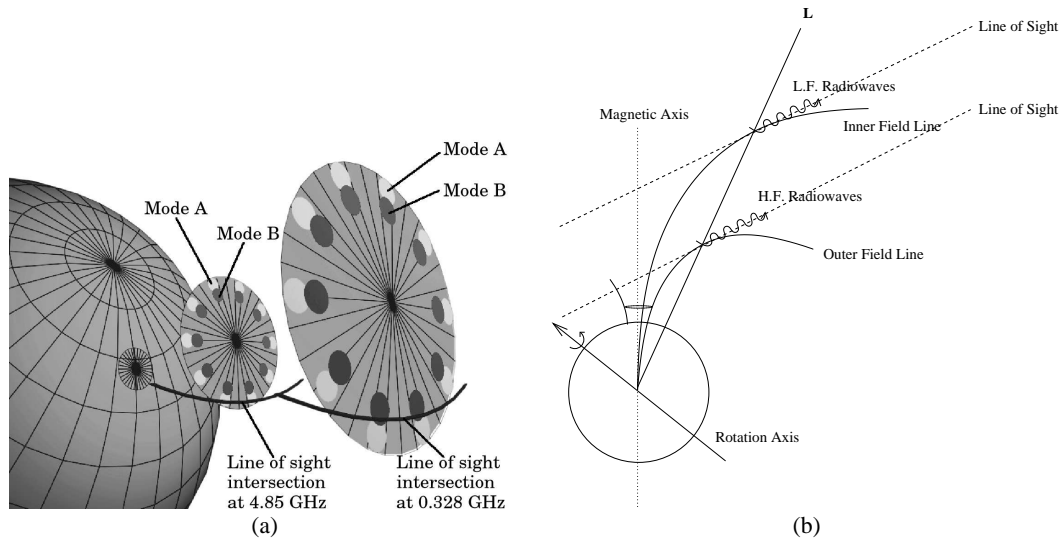


Fig. 4 (a) Schematic overview of the proposed geometrical model to explain the absence of one mode at high frequency. The two large discs are centered around the magnetic axis and represent the emission regions at two different frequencies, corresponding to two different altitudes above the pulsar surface. The smaller circles in the emission region represent the positions of the drifting sub-pulses, which rotate around the magnetic axis. The true number of sub-pulses is unknown. The different drift modes are illustrated by different gray-scales. Note that only one drift mode is assumed to be active at a time. (b) Schematics of two field lines from which radio waves of two different frequencies are observed. L is the line that connects the locations where the field lines are directed towards the observer. Due to radius-to-frequency mapping, low-frequency radio waves are emitted from inner field lines with respect to those where the high-frequency radiation is emitted for the same line of sight.

profile. Figure 3 also shows that the average polarisation of all pulses from the 328-MHz observation has two components and a clear minimum around a pulse phase of 24° . From the average polarisation of pulses at 328 MHz in drift mode A and of those in drift mode B, it is apparent that the pulses in drift mode A contribute only to the component on the left and the pulses in drift mode B contribute only to the component on the right. The average position angle of all pulses shows a 90° jump at both frequencies at a pulse phase of 24° . This can be interpreted as two orthogonally polarised modes changing dominance at this pulse phase. This jump is also visible in the average position angle of pulses that are in mode-B drift. The pulses in mode-A drift only show some degree of linear polarisation in the left part of the profile, just before the mode jump occurs in the average position angle of all pulses. Thus the left part of the A-profile is dominated by one of the two orthogonal polarisation modes, while the lack of polarisation in the right part of the A-profile suggests that here both polarisation modes are of equal strength. The lack of polarisation in the left part of the B-profile suggests that here both polarisation modes are also of equal strength, while the right part of the B-profile is dominated by the other polarisation mode. This means that there is a strong relationship between the drift modes A and B and the two orthogonal modes of polarisation.

3.1 Modelling the Observations

Since the limited length of our observations does not enable us to study mode C, we shall only attempt to model the behaviour of modes A and B, which are the most prominent drift modes. We have found that of these two drift modes only mode A is visible at high frequency, while at low frequency both modes are visible and are seen to have different orthogonal polarisation. At low frequency, the pulses in mode A have less intensity than the pulses in mode B, while at high frequency the pulses show the opposite behaviour. Furthermore, even though the mode B drift is not clearly visible at 4.85 GHz, we do see a hint of 6 seconds periodicity at this frequency. In the context of the potential gap model, the different rates of drift seem

to suggest that the potential gap can take on different stable values. Each stable value can be associated with a particular drift rate and a particular magnetic surface of emission if we assume that the radiation is emitted tangential to the magnetic field lines. An increase in the value of the potential gap is expected to give rise to a faster drift and emission (pair production) from magnetic field-lines closer to the magnetic axis. This leads to the picture of an emission region with two concentric radiating rings. At high frequency, the line of sight intersects with magnetic field lines which are further away from the magnetic axis than at low frequency. Therefore, the drifting component of the inner ring is not seen at high frequency. This is graphically illustrated in Figure 4. Note that when the line of sight is closest to the magnetic axis, mode A is not visible, thus causing a dip in the centre of the A-profile at low frequency.

4 CONCLUSIONS

From an analysis of 2700 pulses from PSR B0031–07 taken simultaneously at 328 MHz and 4.85 GHz we found that from the three known drift modes A, B and C of PSR B0031–07 only mode A is visible at high frequencies. We have constructed a geometrical model that explains how one drift mode can disappear at high frequency while another drift mode remains visible. Further, we have shown that the two most prominent drift modes A and B are associated with two orthogonal modes of polarisation, respectively. To continue the study presented here, one would require more multi-frequency single pulse observations from this pulsar containing full Stokes parameters.

Acknowledgements The authors would like to thank J. Gil for his suggestions and discussion towards interpretation of the results and A. Jessner, A. Karastergiou, B. Stappers and J. Rankin, for their helpful discussions. We also thank all the members of the MFO collaboration for the establishment of the project which led to the observations being available. This paper is based on observations with the 100-m telescope of the MPIfR (Max-Planck-Institut für Radioastronomie) at Effelsberg and the Westerbork Synthesis Radio Telescope (WSRT) and we would like to thank the technical staff and scientists who have been responsible for making these observations possible.

References

- Drake F. D., Craft H. D., 1968, *Nature*, 220, 231
- Manchester R. N., Taylor J. H., Huguenin G. R., 1975, *ApJ*, 196, 83
- Rankin J. M., 1986, *ApJ*, 301, 901
- Smits J. M., Mitra D., Kuijpers J., *A&A*, 440, 683
- Vivekanand M., Joshi B. C., 1997, *ApJ*, 477, 431